Image placement differences between 1:1 projection aligners and 10:1 reduction wafer steppers

William H. Arnold, III

Advanced Micro Devices, Inc., VLSI Technology Development, 901 Thompson Place, Mail Stop 79, Sunnyvale, California, 94086

Abstract

The characteristic image placement errors of both 1:1 projection aligners and 10:1 reduction wafer steppers are studied with reference to the overlay difference between them. Analytical models have been developed in recent years which allow the user of these sophisticated aligners to mathematically identify the many components of pattern-to-pattern registration errors. Using these models and experimental data, it is shown how the mixing of the two types of exposure tool can be done successfully. For the fabrication of present generation devices, it is possible to mix steppers using global alignment capability with 1:1 projection aligners. A realistic production overlay budget is developed for 10:1 steppers, 1:1 projection aligners, and for a process which mixes the two.

Introduction

In the past few years, wafer step-and-repeat systems have begun to replace scanning projection aligners as the photolithographic exposure tool for the fabrication of VLSI devices. Most semiconductor manufacturers now have large numbers of 1:1 projection aligners and a smaller number of wafer steppers, sometimes both in the same fab area. The question naturally arises: Is there some way that the two different types of aligner can be used interchangeably to produce devices?

This paper will examine the technical issues involved in matching the optical image fields of 1:1 scanning projection aligners to that of 10:1 reduction wafer steppers to within the tolerances required for VLSI device fabrication. First, a review of image placement models for both scanning projection aligners and wafer steppers will be given. Then, experimental data will be presented on the range and variability of the characteristic registration errors of both types of systems. Finally, the differences between the way the stepper and the way the 1:1 projection aligner displace image points will be examined.

Review of image placement models

First, let us examine the elementary geometry associated with optical projection systems such as 10:1 wafer steppers and 1:1 scanning projection aligners and define what is meant by perfect overlay of one masking level to the next. Ideally, all the available surface of a silicon wafer should be covered with circuit patterns, the various masking layers of which are aligned at every point perfectly to a reference layer and to each other. In reality, perfect registration is not needed at every point in order to make devices nor is there any physical method of producing and verifying zero error overlay.

Consider the layout of an ideal semiconductor wafer which has many hundreds of individual chips on its surface. The chips are, in general, rectangular and each, with the exception of test sites, are identical in shape and size. These identical units are arranged in a rectilinear array, each separated from its neighbors by scribe lines with widths small in comparison to chip dimensions. The center of each chip is separated from the center of the adjacent one by exact and constant distances in the x and y Cartesian directions.

It is instructive to envision this geometry by imagining a rectilinear lattice of points corresponding to the center of each chip. At each lattice point the chip image is replicated. In the case of the wafer stepper it is usually found that it is most efficient to image more than one chip at a time, so then it is proper to consider the larger rectangular array of chips in the image field and a lattice corresponding to the center points of each field. These concepts are illustrated in Figure 1A.

In reality, detailed position measurements of layer-to-layer registration on wafers, using optical verniers[1,6,8,9], electrical techniques[2,3,5], optical encoder[11], and laser interferometer[4,7] reveal that the rectilinear lattice is distorted and each point is displaced from its ideal location. Following Schneider[1], errors which contribute to the placement error of the center of the chip or field, i.e., the lattice points, will be called grid errors. In addition, it is found that there are further errors in the placement of chip points around the center point. This can result from, for example, lens distortion in

a wafer stepper. Schneider[1] refers to these as column errors when discussing the GCA Model 4800 DSW 10:1 reduction wafer stepper because the origin of these types of errors is in the optical column of the system. To have a more readily identifiable term, however, we will refer to these types of errors as lens errors. Grid and lens errors are graphically illustrated in Figure 1B.

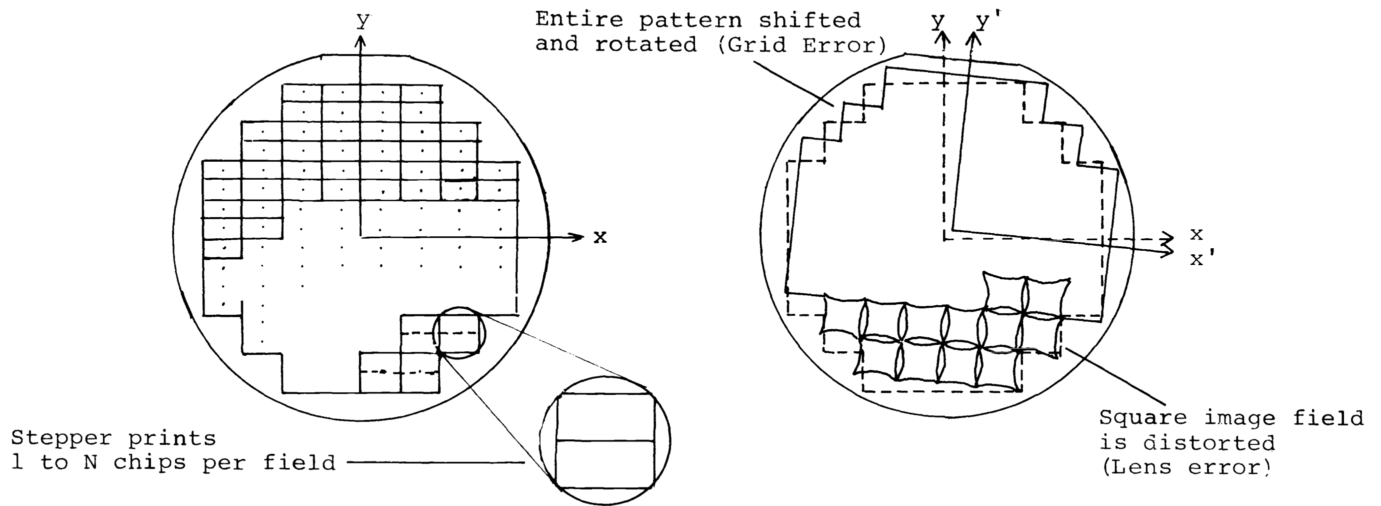

Figure 1A. Ideal rectilinear array of chips. Figure 1B. Effect of grid and lens errors

The various mechanisms by which grid and lens errors can occur in both stepper and 1:1 scanning projection systems will be studied in this paper. An excellent regression model has been developed by Perloff[2,3] and co-workers to characterize grid errors for both 1:1 scanning systems and steppers. Appropriately modified for the specific system, this six parameter model can give very good fit to the experimental data. Vervoordeldonk[5] last year presented here observations and registration data from various models of the Perkin-Elmer 1:1 scanning projection printer. Also presented last year was a regression model similar to Perloff's for lens errors (MacMillen and Ryden[6]) which includes quadratic and cubic terms in field distance. Both models will be used and some small additions will be made in order to describe the total registration error budgets of the systems.

Perloff introduced the six parameters T_x, T_y, θ_x, θ_y, E_x, and E_y to account for translation, rotation, and linear expansion or contraction, respectively, of a second level masking layer aligned to a reference level[2]. Each of these three principal errors is independently estimated in the x and y directions. Differences between the orthogonal components of rotation and expansion can, in many cases, point out characteristic errors other than the three modelled. In stepper systems $(\theta_x-\theta_y)$ signifies an orthogonality error, while in scanning systems it represents cross-scan distortion[5]. The term (E_x-E_y) is associated with the scan distortion of the scanning systems while it has no particular significance except disagreement of x and y scaling in steppers.

Most engineers who work with 1:1 scanning projection systems such as the Perkin-Elmer Micralign will realize that there is a further characteristic distortion of the rectilinear lattice which takes the form of a bowing of the x (scan) and/or y (cross-scan) axes. These bows are easily seen when the grid of the scanning system is compared with that of a stepper with laser-interferometrically guided stages. Experimental characterization of this bow (presented in the next section) has shown a good fit to a parabolic function, hence, the Perloff model will be modified by adding two terms, $B_x y^2$ and $B_y x^2$. The bow coefficients, B_x and B_y, can be set to zero when considering stepper grid errors.

With such a modification, the displacement of the center of each chip (or image field) from its perfect grid point can be represented by the uncoupled equations

$$d_x' = T_x - \theta_x y + E_x x + B_x y^2 \quad (1)$$

$$d_y' = T_y + \theta_y x + E_y y + B_y x^2 \quad (2)$$

In these equations, the calculated displacements in the x and y directions are represented by d_x' and d_y', and x and y refer to the location of the specific chip or field center on the wafer with respect to some origin, in general, different for 1:1 scanning systems and steppers. The coefficients in translation, rotation, expansion, and bow are all calculated from regression analysis using as input the observed displacements d_x and d_y. The residuals $(d_x - d_x')$ and $(d_y - d_y')$ are measures of the portion of the data not fitted and the measurement error. Illustrations of the various types of grid errors for steppers and 1:1 scanning projection systems are given in Figures 2A and 2B (after [2] and [3]). Note that the origin of coordinates for scanning cameras is taken to be the wafer center while the origin in the most common type of wafer stepper is displaced in both directions a sizeable amount from the center of the wafer.

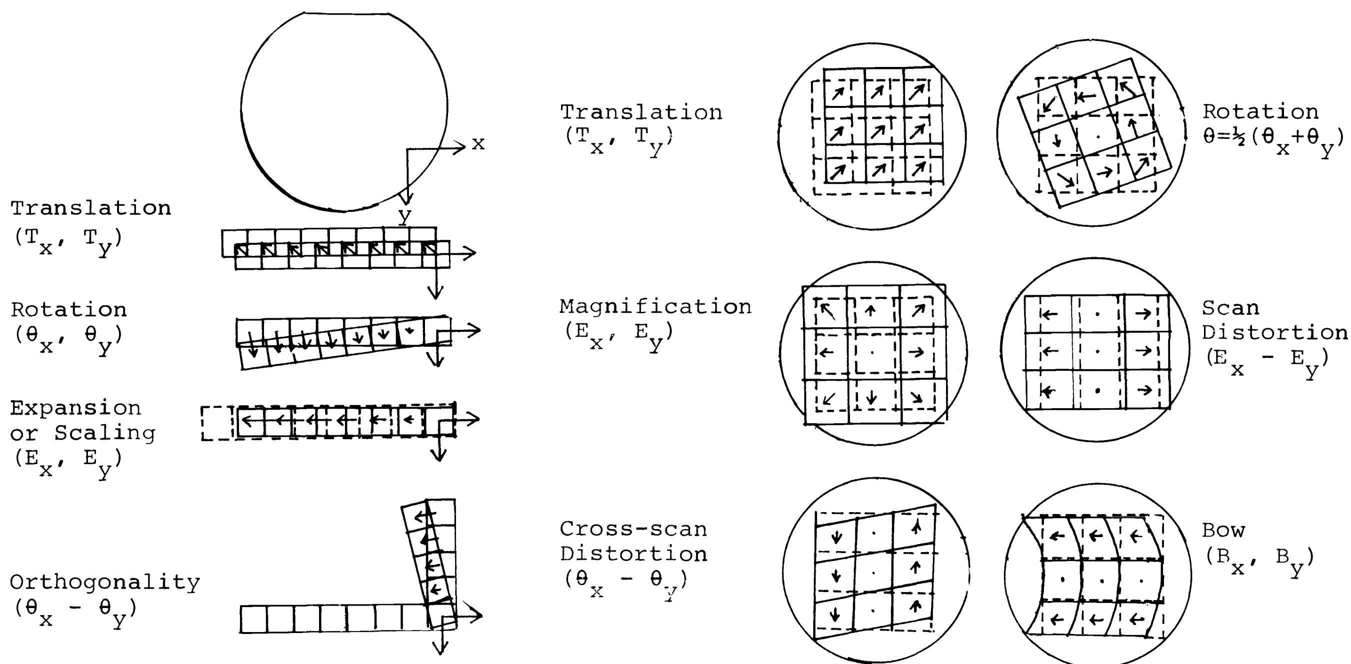

Figure 2A. Grid errors for a 10:1 wafer stepper (System A)

Figure 2B. Characteristic grid errors for a 1:1 scanning projection aligner

In both stepper and scanning systems, lens errors must be considered. It is obvious why this is so for steppers, but is less apparent for 1:1 projection aligners. In many cases, a standard mask making process[7] for 1:1 projection masks is to write a 10X reticle with electron-beam, and then to reduce the reticle image ten times on the chrome mask plate using a mask stepper. The image of the chip as printed on the 1:1 mask plate will already contain image displacements due to errors caused by both the electron-beam writing system and the mask stepper's lens and optical column. Since the electron-beam writing errors will be reduced tenfold upon stepping, the errors due to the mask stepper's optics will usually be dominant.

MacMillen and Ryden[6] have developed a model similar to Perloff's which represents lens errors as combinations of errors of magnification, reticle translation and rotation, trapezoid, and lens distortion. It is revealed that only distortion is intrinsic to the particular lens and that all the rest are related to one or more of the six degrees of freedom of the reticle in the object plane of the stepper's optics. In this model image translation and rotation are treated identically as in the Perloff model, and magnification takes the place of expansion. All calculations take the center of an image field (the grid point) as the origin of coordinates. Trapezoid error involves quadratic terms and lens distortion has cubic terms in the distance perpendicular to the optical axis. The optical axis is taken to be the z-projection through the grid point. These characteristic lens errors are illustrated in Figure 3 [after (6)] as different mechanisms by which the shape, size, location, and orientation of a square image can be changed. Figure 3 also depicts the

relationship between the various errors and the physical degree of freedom from which they arise. For example, magnification errors can result from a Z-translation of the optical column.

The equations for what MacMillen and Ryden[6] call image field placement deviations (IFPD) are:

$$\delta x = \alpha_x + (\Delta M/M)x_o - \theta y_o + t_1 x_o^2 + t_2 x_o y_o - D(x_o^3 + x_o y_o^2) \quad (3)$$

$$\delta y = \alpha_y + (\Delta M/M)y_o + \theta x_o + t_1 x_o y_o + t_2 y_o^2 - D(y_o x_o^2 + y_o^3) \quad (4)$$

where x_o and y_o are the coordinates with the grid point as the origin, the α_i are translation errors, θ describes reticle rotation, $(\Delta M/M)$ is the change of magnification from nominal, t_1 and t_2 are trapezoid parameters, and D measures the intrinsic distortion of the lens.

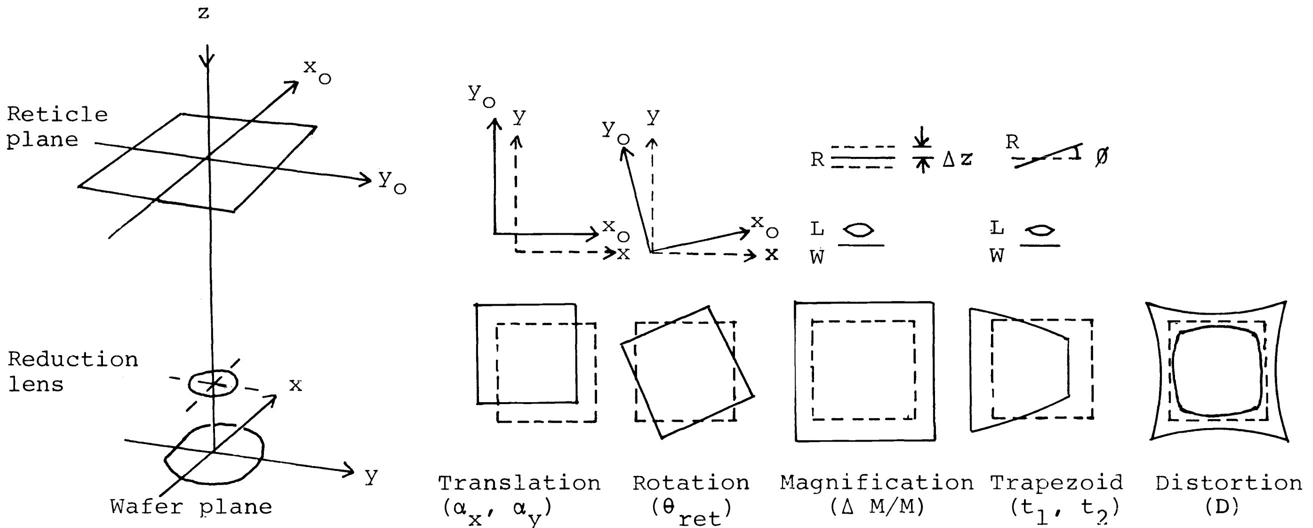

Figure 3. Lens errors

A variety of different situations, ranging from the mapping of a single stepper's lens to the mixed use of a 1:1 projection aligner with a wafer stepper, can be described by an appropriate combination of these two models. The general displacement of a point at location (x_o, y_o) within a field centered at (x, y) from its theoretical position can be written as the sum of the grid error and the lens error

$$\Delta_x = d_x' + \delta x \quad (5)$$

$$\Delta_y = d_y' + \delta y \quad (6)$$

where this can describe, for example, the operation of a wafer stepper or a scanning aligner using a stepper fabricated 1X mask. The magnitude of the displacement is

$$\Delta = (\Delta_x^2 + \Delta_y^2)^{1/2} \quad (7)$$

and the direction of the error is

$$\phi = \tan^{-1}(\Delta_y / \Delta_x) \quad (8)$$

It is difficult to measure (7) for a particular aligner because the equation refers to placement with respect to an ideal rectilinear grid. What one has necessarily is the overlay of two grids, neither of which are ideal. Suppose aligner 1 exhibits vector displacement $\vec{\Delta}_1$ at a given point and aligner 2 has $\vec{\Delta}_2$. The net displacement of the image point in the mixed overlay is $(\vec{\Delta}_1 - \vec{\Delta}_2)$ and this is the quantity measured in machine matching tests.

With such a multiplicity of coefficients, it is no wonder that workers in photolithography are at times at a loss to specify the overlay performance of their aligners

for the circuit designers to work with. In practice, every optical system exhibits small parts of most of the terms in equations 1 - 4. For a particular system, some of the terms in the equations turn out to be negligible, others are almost constant in time (e.g., lens distortion as described by D), and still others can vary significantly over a day, even from one wafer to the next. This combined model characterizes the magnitude and variability of each error and can indicate methods of reducing each in practice. In the next section, some measurements of these coefficients for two common types of 10:1 reduction wafer stepper and two models of a 1:1 scanning projection aligner will be presented.

Most wafer stepper systems now offer some type of "die-by-die" (field-by-field) alignment capability. With this, the stepper can be instructed to align each image field independently of the rest using alignment targets found within the field. In this mode of operation, grid errors are caused only by inaccuracies in the acquisition of the target's signal by the particular detector and, in some systems, by random stage stepping errors due to the requirement of a blind step after target alignment. In most stepper systems and on most device layers, field-by-field alignment significantly reduces the size and range of grid errors so that lens errors become the dominant factor in matching, either one stepper to another or a stepper to a scanning aligner. In the limit of vanishing grid errors, the last major concern in system matching is the precision to which the various lenses to be used are matched. This includes both the lenses used to print the wafer, and the lens used to image the 1X mask for the projection aligner.

The lens matching aspect of mixing wafer steppers and projection aligners has been addressed by Stover and his co-workers[4,8]. In their study they fabricated 1X test masks on mask steppers using Zeiss lenses of the same type (# 107782) as the wafer stepper so that lens matching problems could be held to a minimum. Each wafer was imaged first on a current model 1:1 projection aligner, then aligned field-by-field on the TRE 10:1 wafer stepper. Following this careful procedure they were able to report mixed overlay registration of $\pm$ 0.30 (2σ) on a small sample of wafers. Peavey and co-workers[10] demonstrated grid matching between Perkin-Elmer Model 120 projection aligners and the Optimetrix Model 8010 10:1 wafer stepper, operating in the field-by-field mode, but made no mention of intrafield errors.

It is interesting to see how the characteristic errors of each type of system change as one system is compared against different grids, as defined by the laser interferometer, optical encoder, 1:1 scanning mirror optics or a Zeiss #107782 lens. Of these, the laser interferometer produces the closest approximation to a rectilinear array of equally spaced grid points. Both the lens and the scanning system are subject to linear and nonlinear distortions and that will mask certain features of an overlaid layer and enhance others. An interesting exercise is to separate the first layer error from that of the second and show that the sum is indeed the observed error. This will be demonstrated in the next section for two Zeiss 107782 lenses. It should be noted that the use of a field-by-field alignment system on the second level should produce overlay results at points very close to the theoretical lattice, regardless of the distortion present in the first level aligner. Ideally, the lattice will suffer deformation by random stage errors only.

Experimental results

In this section, data will be presented for the characteristic errors and distortions of both wafer steppers and 1:1 projection aligners. First, typical results obtained when the same aligner is used for both levels are examined. Then the mixing of two aligners of the same type, e.g., 10:1 wafer steppers, will be studied. Finally, data are presented for the matching of a wafer stepper system with a late model 1:1 scanning projection aligner.

Table 1 outlines the important parameters of equations 1-4 and lists estimates of the normal operating range of error attributable to each component for two types of 10:1 wafer steppers and different models of a 1:1 scanning aligner. It should be remembered that in the case of the 1:1 scanning systems, the grid and lens errors inherent in the 1X projection mask used must also be taken into account.

Table 1 - Approximate $\pm 3\sigma$ range of grid and lens coefficients

Grid Errors	Stepper A: Manual Global	Stepper A: Auto Global	Stepper A: Field-by Field	Stepper B: Auto Global	Stepper B: Field-by Field	1:1 Projection: Older Model	1:1 Projection: Newer Model
T_x, T_y = translation error, "offset"	$\pm$0.50μm	$\pm$0.35	$\pm$0.35	$\pm$0.25	$\pm$0.35	$\pm$0.85	$\pm$0.65
θ_x, θ_y = wafer rotation	$\pm$1.00 arc sec*	$\pm$0.65 arc sec	--	$\pm$0.40 arc sec	--	$\pm$2.00 arc sec	$\pm$1.50 arc sec
$(\theta_x - \theta_y)$ = orthogonality, cross-scan distortion	$\pm$0.30 arc sec	$\pm$0.30 arc sec	--	$\pm$0.50 arc sec	--	$\pm$1.25 arc sec	$\pm$0.75 arc sec
E_x, E_y = expansion, magnification	$\pm$1.00ppm	$\pm$1.00ppm	--	$\pm$1.50ppm	--	$\pm$10ppm	$\pm$5ppm
$(E_x - E_y)$ = scan distortion	$\pm$1.00ppm	$\pm$1.00ppm	--	$\pm$1.50ppm	--	$\pm$8ppm	$\pm$3ppm
B_x, B_y = bow	--	--	--	--	--	$\pm 3.5 \times 10^{-4}$ um/mm^2	$\pm 2 \times 10^{-4}$ um/mm^2
σ_{sx}, σ_{sy} = random stage errors	$\pm$0.10μm	$\pm$0.10	$\pm$0.10	$\pm$0.25	--	--	--

*1 arc sec = 4.848ppm

Lens errors	(Zeiss 107782)	(Tropel 1068GH)
θ_{ret} = field rotation	$\pm$ 7 arc sec	$\pm$ 6 arc sec
$(\Delta M/M)$ = magnification	$\pm$ 30 ppm	$\pm$ 35 ppm
t_1, t_2 = trapezoid	$\pm$ 4×10^{-3} μm/mm^2	$\pm$ 3×10^{-3} μm/mm^2
D_x, D_y = lens distortion	$\pm$ 1×10^{-3} um/mm^3	$\pm$ 1×10^{-3} um/mm^3
σ_{fx}, σ_{fy} = random field size changes	$\pm$0.10um (at field boundary)	$\pm$0.30um (at field boundary)

T_x = .12μm
T_y = .10μm
θ_x = -2.77ppm
θ_y = -3.40ppm
E_x = -.26ppm
E_y = -2.25ppm
S_x = .05μm
S_y = .05μm
r_x^2 = .79
r_y^2 = .82

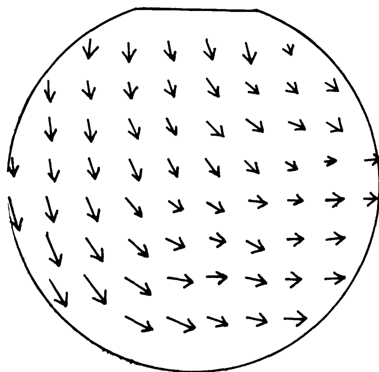

Scale
0.50μm

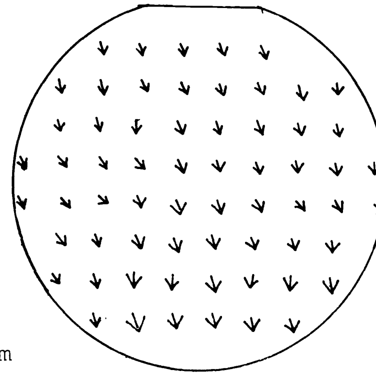

T_x = .04μm
T_y = .09μm
θ_x = .12ppm
θ_y = .10ppm
E_x = .19ppm
E_y = .09ppm
S_x = .03μm
S_y = .03μm
r_x^2 = .90
r_y^2 = .93

Figure 4A. 1:1 scanning aligner - both layers

Figure 4B. 10:1 wafer stepper (System A2) - both layers

Figure 4A shows a vector map of a wafer with both layers aligned by the same late-model 1:1 projection printer and Figure 4B, a wafer with both layers imaged by a 10:1 stepper employing manual global alignment. The data represented in Figures 4A and 4B were gathered using an electrical resistance measurement of misregistration, similar to those described by Perloff[2] and other places. From these we see that level-to-level grid overlay of a system to itself, either stepper or scanning aligner, can be good to $\pm$0.35 micron.

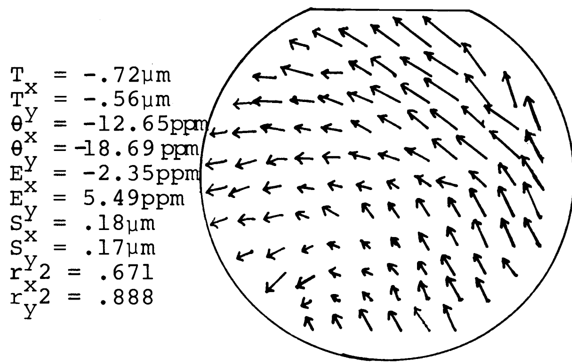

Scale

2.0µm

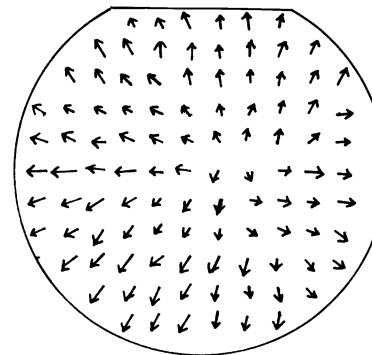

T_x = .19µm
T_y = .17µm
θ_x = .23ppm
θ_y = .10ppm
E_x = 7.03ppm
E_y = 7.89ppm
S_x = .07µm
S_y = .06µm
r_x^2 = .911
r_y^2 = .931

Figure 5A. Mixed 1:1 scanning aligners

Figure 5B. Mixed 10:1 wafer steppers: Systems A1, A2

The result of mixing two 1:1 projection aligners is pictured in Figure 5A. Figure 5B shows the grid matching of two similar wafer stepper systems. In both of these there is degradation in comparison with the previous case of a single system used for both layers. In the stepper case, grid matching can be adjusted through computer software so that a very close fit between two systems can be achieved at any point in time. The isotropic scaling error of approximately 7 parts per million found in the wafer of Figure 5B is a particularly simple error to measure and correct. The cameras tend to drift away from the fit in times short compared with the average length of a VLSI wafer process. Hence, most wafer stepper users calibrate their instruments with a set of reference wafers, printed originally on one of the systems at the time of the system matching.

A true picture of how a stepper's reduction lens distorts a square grid is difficult to determine using some manufacturer's standard tests[9] for lens errors. Indeed, as MacMillen and Ryden[6] point out, this test does not measure all the coefficients found in equations 3 and 4 (neglecting two of four trapezoid parameters and one component of reticle rotation). A particularly simple way to test a stepper's lens and optical set-up is to command the system to compare the placement of points within the field by the optics against a rectilinear grid defined by the stage positioning mechanism, either laser interferometer or optical encoder, and the image at field center, where there is the least error due to magnification and distortion. This basic idea occurred to at least five groups last year[4,6,7,13] and this author. In the two stepper systems considered in this study, this can be done by stopping down the field to expose only a single male vernier at the optical axis. This vernier is then stepped to form a rectilinear grid with verniers spaced distances x and y apart. The image field is then opened fully to expose female verniers spaced every 10x and 10y on the reticle. This full field of females is reduced and stepped exactly to interlock with the rectilinear male grid. This is illustrated in Figures 6A and 6B.

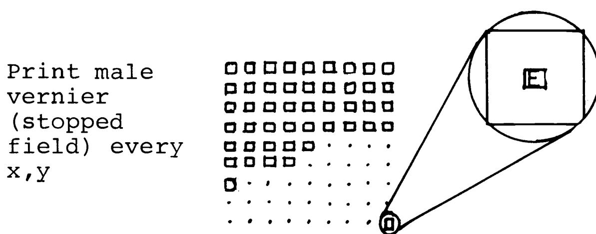

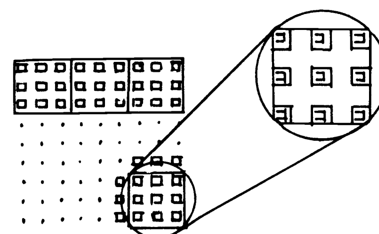

Print 9 females (full field) every 3x,3y

Figure 6A. Definition of a rectilinear grid by stepper stage and optical axis

Figure 6B. Comparison of the lens with the grid

Tests of this kind have produced the first two lens maps shown in Figure 7A and 7B. The lenses are Zeiss 107782 10:1 reduction lenses mounted in Manufacturer A's system. The measurements were taken at nine points in the field, one in the center and eight arranged on the boundary of an 8.6mm square. These maps are drawn such that the error at field center is zero. System A2 exhibits a classic pincushion distortion and a fair amount of rotation

while system A1 shows large trapezoid errors in the upper part of its field. Upon subtracting the data of system A2 from that of system A1, the map of Figure 7C is found. The rotation in system A2 and trapezoid in system A1 have added to make the error in the upper right and left corners approach 0.50um. Experimental verification that this method of measuring lens errors and mathematically deducing the result of mixed lens overlay is shown in Figure 7D. This map is the result of imaging a full field of female verniers on system A1 and interlocking these with an identical full field male image printed by system A2.

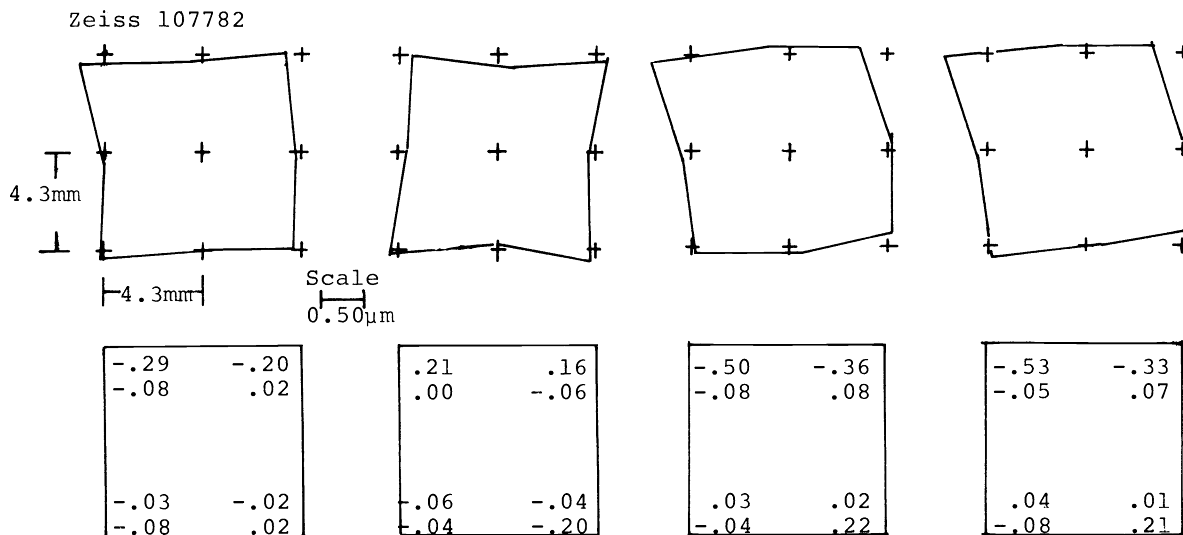

Figure 7A. Lens map: System A1
Figure 7B. Lens map: System A2
Figure 7C. Vector subtraction (A1-A2)
Figure 7D. Measured mixed overlay: A1, A2

The question of whether a certain lens can be matched to another is simply answered once maps of this type have been constructed for both lenses. This study has found that there are no inherent problems in matching lenses from different manufacturers, as long as care is taken to base each system's stage scaling on a common reference. It was shown last year that grid matching of 10:1 wafer steppers from different manufacturers is achievable.[11] Lenses from the same two instruments can now be compared. In Figure 8A the lens map of a Tropel #1068GH 10:1 microreduction lens mounted in Manufacturer B's system is shown. The matching between this lens and the Zeiss lens shown in Figure 7B is shown in Figure 8B.

There are small random components to grid and lens errors in stepper systems. Simple stage precision tests can be run to measure the random error component of grid errors. Electrical measurements of random stage positioning error for the three stepper systems of Figures 7A, 7B, and 8A were as follows: (300 pts. per system)

System	$\pm 3\sigma_x$ (um)	$\pm 3\sigma_y$ (um)
A1	$\pm$ 0.099	$\pm$ 0.063
A2	$\pm$ 0.087	$\pm$ 0.054
B1	$\pm$ 0.270	$\pm$ 0.256

The laser interferometer is clearly superior to the optical encoder in terms of measurement precision. Recently Rottmann[12] published data which shows that small uncontrolled focus changes in a mask stepper can give rise to variations in the printed field size. Using the same technique as for lens mapping, the four corner points and four axial points on the periphery of a 8.6mm square field were measured for 120 separate fields printed by systems A2 and B1. After subtracting the random error found at the field center (which corresponds to the stage precision) from that at each of the eight field boundary points, the data presented in Figure 9 was found. In this figure, each set of two numbers

represents the $\pm 1\sigma$ x and y random error found at that point. It can be seen that points at the boundary of a stepper's image field will suffer random errors of range ± 0.10 micron in system A and ± 0.30 micron in system B. As Rottmann suggests, experimental evidence shows that the major cause of these errors are changes in the magnification ratio due to small variations in the focus setting of the camera. Another component of the error is due to yawing of the optical column during stepping. To estimate the range of focus variation necessary to produce random field size errors of these sizes, experiments were run in which the lens map of the stepper was measured at different focus settings, using the test previously described. Figures 10A and 10B show how the magnification coefficient of eqn. 4 $(\Delta M/M)_y$ changes as the focus setting is varied in systems A and B. In both cases, the zero of the focus was determined by measuring the linewidth of nominal 2.0 micron lines as a function of exposure and focus and finding the common extremum of the curves. This is the stepper equivalent of Bossung[15] curves, the well-known procedure for determining best imaging focus in the 1:1 scanning projection aligner. In a perfect 10:1 wafer stepper, both 10:1 reduction ratio and best imaging focus should occur at the same point, and the slope of magnification versus focus should be as small as theoretically possible.

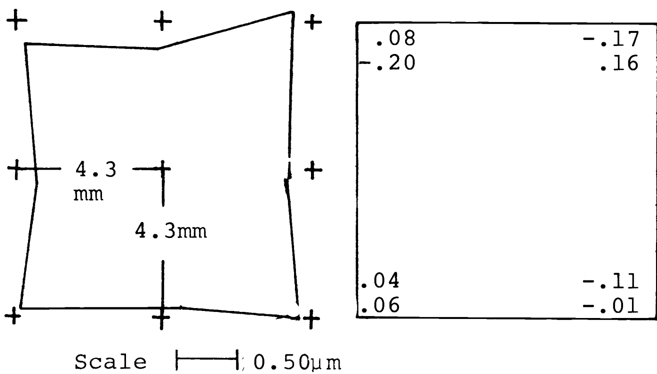

Figure 8A. Lens map: System B1 (Tropel 1068GH)

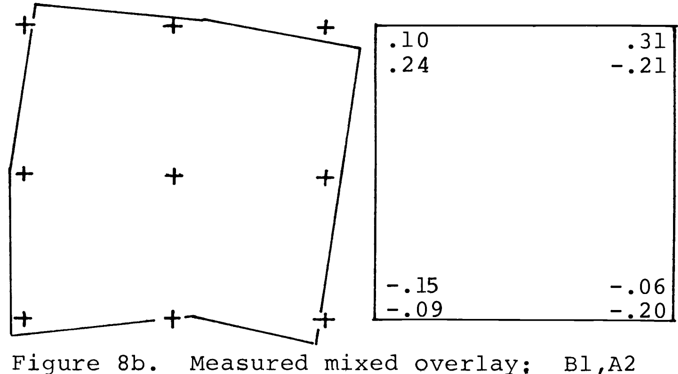

Figure 8b. Measured mixed overlay: B1,A2

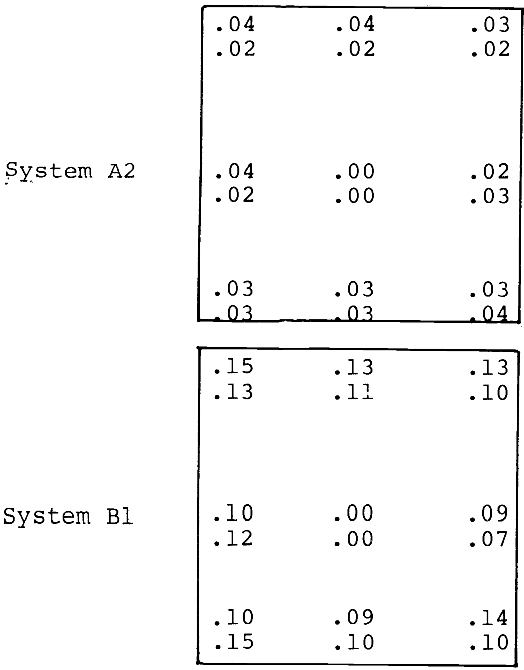

Figure 9. Random field size changes ($\pm 1\sigma$) - (um)

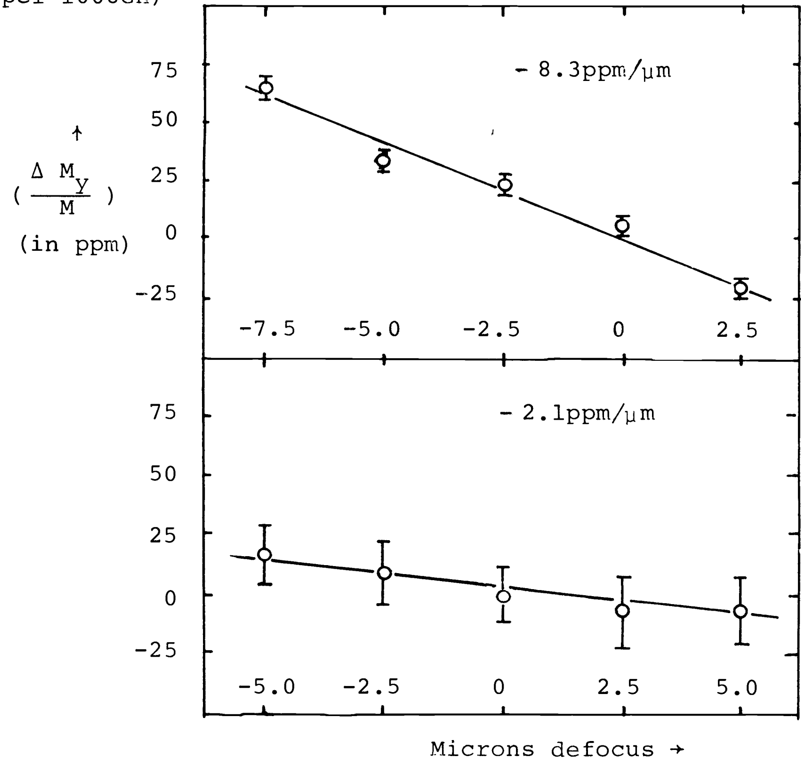

Figure 10A. Change of magnification with focus setting: System A1

Figure 10B. System B1

The comparison of the full wafer image field of the 1:1 scanning projection aligner with the rectilinear grid of the wafer stepper yields interesting insights into the characteristic distortion of the former. In this study, two sets of matched 1X masks and 10X reticles were used, one in which test structures were printed for electrical evaluation of misregistration, the other employing optical verniers. Both sets of 1X plates were printed by a mask stepper with a Zeiss 107782 lens.

Wafer steppers can be operated in a variety of alignnment modes, ranging from manual two-point (global) alignment to automatic field-by-field alignment, with several gradations in between. The vector map of Figure 11A shows a wafer aligned first on an intermediate model 1:1 scanning aligner then on wafer stepper system A2, operated in the manual global mode (i.e., only T_x, T_y, θ_x, and θ_y adjusted during wafer alignment). Readings were taken from 100 optical verniers spaced at 7.5mm in each direction. As compared against the laser grid of the stepper, the 1:1 scanning field is apparently bowed, with points along the y-axis displaced in x progressively more as the distance from wafer center increases. The largest vector length found on this wafer was 0.79 micron. A very similar map to this was published last year by Vervoordeldonk et.al.[14], comparing the Philips wafer stepper and the Perkin-Elmer 1:1 aligner. Histograms for this data, as well as the calculated coefficients, using the Perloff model only (i.e. without B_x or B_y), are given in Figure 11B. The very poor multiple correlation coefficient of $r_x^2 = 0.115$ for x directed errors indicates that some further mechanism is at work. Figure 11C compares an average of the y-bow measured by column versus the calculated parabola with $B_x = -3.05 \times 10^{-4} um/mm^2$.

Figure 12A depicts the results of a wafer aligned first on a late model 1:1 scanning aligner and then on the same stepper as before (A2). This time the electrical test mask set was used. In this case there is a considerable scaling error in both the x and y directions (E_x = -3.35 parts per million-ppm, E_y = 9.79 ppm). This error was traced to two main sources. First, it was determined that there was a 3 ppm isotropic scaling difference between System A2 and the mask stepper used to print the 1X plate. The second source was found to be sizeable scaling differences between the set of reference wafers used to calibrate the steppers and the similar, but uncorrelated set of wafers for the scanning aligners. After subtracting away the part of the data accounted for by T, θ, and E, the residuals at each point are shown in Figure 12B. Inspecting this map carefully, both an x and a y bow can be seen ($B_x = -1.00 \times 10^{-4} um/mm^2$, $B_y = -1.26 \times 10^{-4} um/mm^2$).

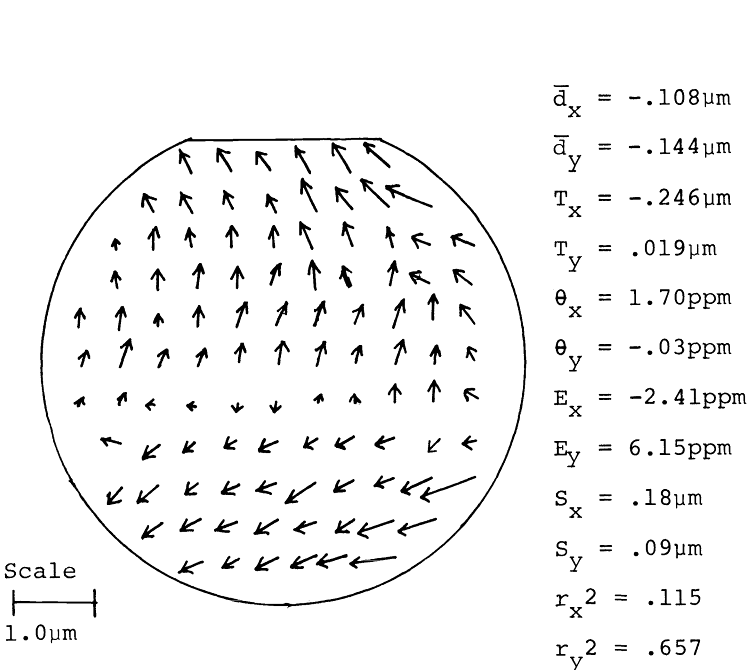

Figure 11A. Full wafer grid overlay 10:1 wafer stepper and 1:1 scanning projection aligner

Percent of Measurements

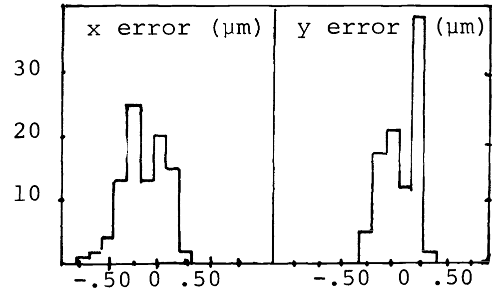

Figure 11B. Histograms

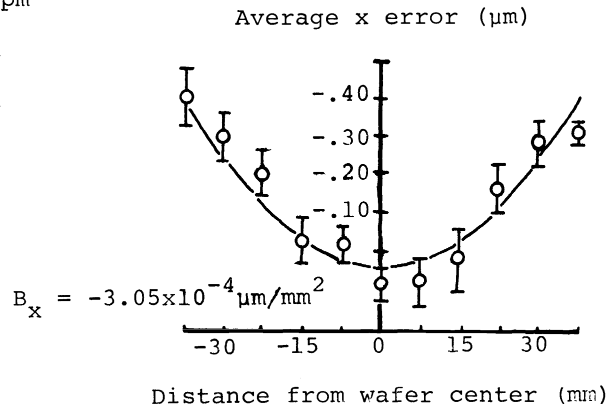

Figure 11C. Parabolic fit to bow

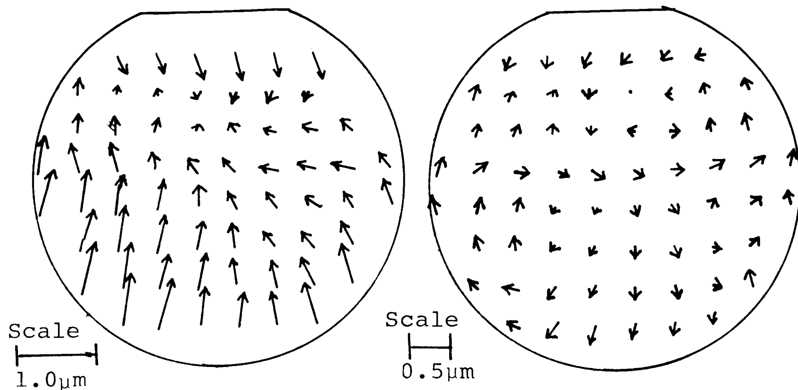

Figure 12A. Raw data; Figure 12B. Residual bow Electrical measurement of grid overlay: 10:1 wafer stepper and 1:1 scanning aligner - 2 point global alignment

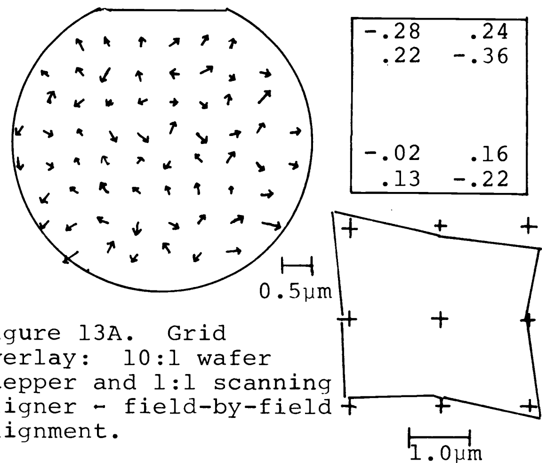

Figure 13A. Grid overlay: 10:1 wafer stepper and 1:1 scanning aligner - field-by-field alignment.

Figure 13B. Field matching

In scanning projection printers there can be random field size changes also, which result from small perturbations of the magnification ratio about unity. The most common cause of magnification error in the scanning aligner is the differential heating of the 1:1 projection mask and wafer. In this case, the entire grid will expand or contract and the individual fields will suffer the same fractional (ppm) error as the grid. Eight wafers of which the wafer of Figure 12A was one, in which the projection printer was compared against the stepper grid had average x and y expansion coefficients of

$$E_x = -2.34 \pm 1.43 \text{ ppm } (\pm 1\sigma)$$

$$E_y = 10.32 \pm 1.33 \text{ ppm } (\pm 1\sigma)$$

Noise level expansion error on System A2 for wafers run at the same time has been measured as approximately $\pm$ 0.40 ppm (1 σ) along both axes. Thus random magnification changes in this series of wafers amounted to approximately $\pm$1.2ppm (rms).

When the stepper is operated in the field-by-field mode in aligning to a wafer previously printed on a scanning projection aligner, grid errors are reduced to a minimum. Figure 13A shows the result of mixed overlay between System B1 and a late model 1:1 scanning aligner, where the stepper aligned each field independently of the rest. Figure 13B shows the field matching found. The largest vector grid error found was 0.36 micron and the largest error found within the field was 0.42um.

Discussion and conclusions

The mixed overlay of 1:1 projection aligners and reduction wafer steppers can be analyzed in a straightforward fashion using presently available models. Through proper characterization and careful tuning, the process engineer can mix the two types of aligners to produce VLSI devices. Depending on the registration tolerance of the particular device, the stepper can be used in either two point global alignment mode or in field-by-field mode.

When global alignment is used, serious problems can result from gross mismatches in characteristic grid errors. The worst mismatch found by this study results from the way the scanning aligner bows parallel lines along the x and y axes. Image placement differences between stepper and scanning aligners due to bow only can be as much as $\pm$1 micron over a four inch wafer for older models, but is reduced considerably for newer models. Another serious problem can occur from severe scan distortion in the scanning aligner because wafer stepper systems typically measure scaling only along the x-axis. If the scaling error along the y-axis is significantly different from that along x, the automatic isotropic compensation usually made will actually result in worse overlay.

When field-by-field alignment is used, grid errors are reduced to the order of the stage precision error. At this point, the error contribution of the lenses involved becomes dominant. To make mixing of steppers and scanning aligners work well, the lenses used to print the 1X projection masks and the stepper lenses must be matched. The best case would

be if the same stepper is used to print the 1X projection masks and step the wafers, though this is probably unrealistic. The question of how well the stepper can align to an electron-beam fabricated 1X mask plate was not studied.

Wafer steppers offer superior resolution, registration, and yield potential, while scanning aligners have greater throughput rates and are the standard lithographic tool in most device fabrication areas. The ability to use them interchangeably on the same product would be of obvious utility and there might be an economic advantage involved. The results of this study suggest that the mixing of the two types of aligners can be done successfully and offers a middle ground in overlay accuracy between that of just scanning aligners or steppers exclusively.

Acknowledgements

I would like to thank Sue Powell, Anna Minvielle, and Anita Schnupp of VLSI Technology Development and Dave Pearson of SRAM Design for their help in design and implementation of the test masks and in collecting the data presented here.

References

1. W.C. Schneider, Intermachine Registration Errors of Wafer Step-and-Repeat Systems, SPIE Semiconductor Microlithography V, Vol. 221, p. 26, 1980.
2. D.S. Perloff, A Four-Point Electrical Measurement Technique for Characterizing Mask Superposition Errors on Semiconductor Wafers, IEEE J. Sol. St. Circ., Vol. SC-13, No. 4, pp. 436-444, August, 1978.
3. T.F. Hasan, S.U. Katzman, D.S. Perloff, Automated Electrical Measurements of Registration Errors in Step-and-Repeat Optical Lithography Systems, IEEE Trans. El.Dev., Vol. ED-27, No. 12, pp. 2304-2312, December, 1980.
4. C. Van Peski, Minimizing Pattern Registration Errors Through Wafer Stepper Matching Techniques, Solid St. Tech., Vol. 25, No. 4, p. 111, April, 1982.
5. R. Vervoordeldonk, P. Willemse, R. Kramer, Registration Accuracy in Several Versions of a Scanning 1:1 Optical Projection System, SPIE Vol. 334 Optical Microlithography, pp. 26-33, 1982.
6. D. MacMillen, W.D. Ryden, Analysis of Image Field Placement Deviations of a 5X Microlithographic Reduction Lens, SPIE Vol. 334 Optical Microlithography, pp. 78-89, 1982.
7. S.K. Dunbrack, G. Burns, Electron Beam vs. Optical Step-and-Repeat: A 10X Reticle and 1X Die Distortion Study Employing Nikon X-Y Laser Interferometric Metrology, SPIE Vol. 334 Optical Microlithography, pp. 219-229, 1982.
8. H.L. Stover, N.E. David, T.H. Lewis, Mix-and Match of 10:1 Wafer Steppers With Die-by-Die Alignment to 1:1 Proximity and Projection Systems, Solid St. Tech., Vol. 25, No. 10, pp. 124-132, October, 1982.
9. W.C. Schneider, Testing the Mann Type 4800DSW™ Wafer Stepper™, SPIE Vol. 174 Developments in Semiconductor Microlithography IV, pp. 6-14, 1979.
10. J.H. Peavey, S. Cosentino, C. Hammer, Hybrid Lithography: Mixing of 10:1 and 1:1 Projection Aligners, SPIE Vol. 334, pp. 149-156, 1982.
11. A. Stephanakis, H. Coleman, Mix and Match - 10X Reduction Wafer Steppers, SPIE Vol. 334, pp. 132-138, 1982.
12. H.R. Rottmann, Metrology in Mask Manufacturing, IBM J. Res. Develop, Vol. 26, No. 5, pp. 553-560, September, 1982.
13. S.C. Curry, C.B. Friedberg, Wafer Stepper Characterization and Process Control Techniques, SPIE Vol. 334, pp. 105-110, 1982.
14. R. Kramer, R. Vervoordeldonk, S. Wittekoek, R. Beam, G. Van der Looij, Philips Wafer Stepper: Characterization and Processing Experience, SPIE Vol. 334, pp. 95-104, 1982.
15. J.W. Bossung, Proc. Soc. Photo-Optical Instrum. Eng., Vol. 100, p. 80, April, 1977.